Nonperturbative analysis of nuclear shape effects on the bound electron g factor

Niklas Michel,[*] Jacek Zatorski, Natalia S. Oreshkina, and Christoph H. Keitel
Max Planck Institute for Nuclear Physics, Saupfercheckweg 1, 69117 Heidelberg, Germany

(Received 1 June 2018; published 8 January 2019)

The theory of the g factor of an electron bound to a deformed nucleus is considered nonperturbatively and results are presented for a wide range of nuclei with charge numbers from Z=16 up to $Z = 98$. We calculate the nuclear deformation correction to the bound electron g factor within a numerical approach and reveal a sizable difference compared to previous state-of-the-art analytical calculations. We also note particularly low values in the region of filled proton or neutron shells, and thus a reflection of the nuclear shell structure both in the charge and neutron number.

DOI: 10.1103/PhysRevA.99.012505

I. INTRODUCTION

The electron's g factor characterizes its magnetic moment in terms of its angular momentum. For an electron bound to an atomic nucleus, the g factor can be predicted in the framework of bound-state quantum electrodynamics (QED) as well as measured in Penning traps, both with a very high degree of accuracy. This enables extraction of information on fundamental interactions, constants, and nuclear structure. For example, the combination of theory and precise measurements of the bound electron g factor has recently provided an improved value for the electron mass [1], and bound-state QED in strong fields was tested with unprecedented precision [2–5]. It also enables measurement on characteristics of nuclei such as electric charge radii, as shown for the Si^{13+} ion [6], or the isotopic mass difference as demonstrated for ^{48}Ca and ^{40}Ca in [7], or, as proposed theoretically, magnetic moments [8,9]. Also, it was argued that g-factor experiments with heavy ions could result in a value for the fine-structure constant which is more accurate than the presently established one [10,11]. With planned experiments involving high-Z nuclei [12–14] and current experimental accuracies on the 10^{-10} level for low Z, it is important to keep track also of higher order effects. In this context, besides one-loop QED [15,16], which is well under control, two-loop QED [17–20], which requires further investigation, and nuclear polarization [21,22], also the influence of nuclear size [23,24] and shape is critical. In Ref. [25], the nuclear shape correction to the bound electron g factor was introduced and calculated for spinless nuclei using the perturbative effective radius method (ERM) [26,27]. This effect takes the influence of a deformed nuclear charge distribution into account and changes the g factor up to the 10^{-6} level for heavy nuclei, and thus is potentially visible in future experiments. Additionally, the uncertainty of the finite nuclear size correction to the Lamb shift in hydrogenlike ^{238}U was shown to be sensitive to nuclear deformation (ND) effects [27]. This motivates the possibility of lowering uncertainties for the bound electron g factor by considering ND. Therefore, a comparison of experiment and theory for heavy nuclei demands a critical scrutiny of the validity of the previously used perturbative methods, as pointed out in Ref. [28].

In this paper, we present nonperturbative calculations of the ND correction to the bound electron g factor and show the corresponding values for nuclei across the entire nuclear chart, quantifying the nonperturbative corrections and especially observing the appearance of nuclear shell closure effects in the values of the bound electron g factor.

Relativistic units with $\hbar = c = 1$ are used throughout this work, as well as the Heavyside unit of charge with $\alpha = e^2/4\pi$, where α is the fine structure constant and the elementary charge e is negative.

II. AVERAGED NUCLEAR POTENTIAL

It has been shown in Ref. [27] that for spinless nuclei the relativistic Hamiltonian for the electron bound to a deformed nucleus reads

$$\mathrm{H}_e = \vec{\alpha} \cdot \vec{p} + \beta m_e + V(r). \tag{1}$$

Here, $\vec{\alpha}$ and β are the four Dirac matrices, $\vec{p}$ is the electron's momentum, m_e is the electron mass, and the electric interaction between eletron and nucleus can be described in terms of the nuclear charge distribution $\rho(\vec{r})$ as

$$V(r) = -Z\alpha \int d^3r' \, \frac{\rho(\vec{r}\,')}{r_>}, \tag{2}$$

where $r_> := \max(r, r')$. For spherically symmetric charge distributions, this leads to finite-size effects in atomic spectra [26]. However, it is important to note that this formula is also valid for deformed nuclear charge distributions, although the resulting potential is spherically symmetric. The solution of the corresponding eigenvalue equation

$$\mathrm{H}_e|n\kappa m\rangle = E|n\kappa m\rangle \tag{3}$$

can be written in position space in terms of the well-known spherical spinors $\Omega_{\kappa m}(\vartheta, \varphi)$ and the radial functions $G_{n\kappa}(r)$, $F_{n\kappa}(r)$ [29] and depends on the principal quantum number n, the relativistic angular momentum quantum number κ, and the z component of the total angular momentum m.

[*]niklas.michel@mpi-hd.mpg.de

In this work, we focus on quadrupole and hexadecapole deformations, since atomic nuclei do not possess static dipole moments. Here, the deformed Fermi distribution

$$\rho_{ca\beta_2\beta_4}(r,\vartheta) = \frac{N}{1+\exp\left(\frac{r-c(1+\beta_2 Y_{20}(\vartheta)+\beta_4 Y_{40}(\vartheta))}{a}\right)} \quad (4)$$

as a model of the nuclear charge distribution has proved to be very successful, e.g., in heavy muonic atom spectroscopy with deformed nuclei [30,31]; the normal Fermi distribution ($\beta_2 = \beta_4 = 0$) has also been used in electron-nucleus scattering experiments determining the nuclear charge distribution [32]. Here, a is a skin thickness parameter and c is the half-density radius, while β_2, β_4 are the quadrupole and hexadecapole deformation parameters, respectively. $Y_{lm}(\vartheta,\varphi)$ are the spherical harmonics and $Y_{l0}(\vartheta)$ depend only on the polar angle ϑ, not on the azimuthal angle φ. The normalization constant N is determined by the condition

$$\int d^3r\, \rho_{ca\beta_2\beta_4}(r,\vartheta) = 1. \quad (5)$$

III. NUCLEAR DEFORMATION CORRECTION TO THE g FACTOR

In an external, homogeneous, and weak magnetic field $\vec{B}$, the g factor of the bound electron is defined by the first-order energy splitting δE due to the external field as the proportionality coefficient [33]

$$\delta E = -e\,\langle n\kappa m|\vec{\alpha}\cdot\vec{A}|n\kappa m\rangle =: m\, g\, \mu_B|\vec{B}|, \quad (6)$$

where $\vec{A} = \frac{1}{2}[\vec{B}\times\vec{r}\,]$ is the corresponding vector potential and μ_B is the Bohr magneton. The g factor in central potentials is independent of the quantum number m. It can be expressed in terms of the radial functions as

$$g = \frac{2m_e\kappa}{j(j+1)}\int_0^\infty dr\, r\, G_{n\kappa}(r)\, F_{n\kappa}(r), \quad (7)$$

where $j = |\kappa| - 1/2$ is the total angular momentum of the electron. Alternatively, the bound electron g factor can be expressed for arbitrary central potentials in terms of the derivative of the eigenenergies with respect to the electron's mass [34] as

$$g = -\frac{\kappa}{2j(j+1)}\left(1 - 2\kappa\frac{\partial E_{n\kappa}}{\partial m_e}\right). \quad (8)$$

For the model of a pointlike nucleus, the radial wave functions are known analytically and the ground-state g factor with $n = 1$ and $\kappa = -1$ is

$$g_{\text{point}} = \tfrac{2}{3}(1+2\gamma), \quad (9)$$

with $\gamma = \sqrt{1-(Z\alpha)^2}$, a result presented for the first time by Breit [35]. For the deformed Fermi distribution (4) with a fixed charge number Z, the g factor (7) is completely determined by the parameters c, a, β_2, and β_4, and therefore can be written for the ground state as

$$g = g_{\text{point}} + \delta g_{\text{FS}}^{(ca\beta_2\beta_4)}, \quad (10)$$

where $\delta g_{\text{FS}}^{(ca\beta_2\beta_4)}$ is the finite-size correction depending on the parameters c, a, β_2, and β_4. In Ref. [25], the ND correction to the bound electron g factor is defined as the difference of the finite-size effect due a deformed charge distribution and due to a symmetric charge distribution (i.e., $\beta_2 = \beta_4 = 0$) with the same nuclear radius as

$$\delta g_{\text{ND}} = \delta g_{\text{FS}}^{(c_1 a\beta_2\beta_4)} - \delta g_{\text{FS}}^{(c_2 a 00)}, \quad (11)$$

where $a = 2.3\,\text{fm}/[4\ln(3)]$, and c_i are determined such that $\sqrt{\langle r^2\rangle_\rho}$ of the corresponding charge distribution agrees with the root-mean-square (rms) values from literature [36]. The nth moment of a charge distribution $\rho(\vec{r}\,)$ is defined as

$$\langle r^n\rangle_\rho = \int d^3r\, r^n \rho(\vec{r}\,). \quad (12)$$

Values for the deformation parameter β_2 can be obtained by literature values of the reduced $E2$-transition probabilities from a nuclear state ${2^+}_i$ to the ground state 0^+ via [37]

$$\beta_2 = \frac{4\pi}{3Z|e|\sqrt{5\langle r^2\rangle_\rho/3}}\left[\sum_i B(E2; 0^+ \to {2^+}_i)\right]^{1/2}, \quad (13)$$

and estimates for β_4 can be found in Ref. [38]. From Eq. (11), it is evident that the ND correction is a difference of two finite-size effects and therefore especially sensitive to higher order effects. However, for high Z it reaches the 10^{-6} level and therefore is very significant.

It was shown in [25] with the ERM [26] that $\delta g_{\text{FS}}^{(ca\beta_2\beta_4)}$ and therefore δg_{ND} mainly depends on the moments $\langle r^2\rangle_\rho$ and $\langle r^4\rangle_\rho$. δg_{ND} can be calculated with the formula [34]

$$\delta g_{\text{FS}}^{(ca\beta_2\beta_4)} = \frac{4}{3}\frac{\partial E_{\text{FS}}(c,a,\beta_2,\beta_4)}{\partial m_e}, \quad (14)$$

which is a direct consequence of Eq. (8) and where $E_{\text{FS}}(c,a,\beta_2,\beta_4)$ is the energy correction due to $\rho_{ca\beta_2\beta_4}(r,\vartheta)$ compared to the pointlike nucleus. The effective radius R is defined as the radius of a homogeneously charged sphere with the same energy correction $E_{\text{FS}}^{(\text{sph})}(R)$ as the deformed Fermi distribution via

$$E_{\text{FS}}^{(\text{sph})}(R) = E_{\text{FS}}(c,a,\beta_2,\beta_4). \quad (15)$$

The energy correction can be approximated [26] as

$$E_{\text{FS}}^{(\text{sph})}(R) \approx \frac{(Z\alpha)^2}{10}[1+(Z\alpha)^2 f(Z\alpha)](2Z\alpha R m_e)^{2\gamma} m_e. \quad (16)$$

Here, $f(x) = 1.380 - 0.162x + 1.612x^2$ and the effective radius is approximately

$$R \approx \sqrt{\frac{5}{3}\langle r^2\rangle_{\rho_{ca\beta_2\beta_4}}\left[1 - \frac{3}{4}(Z\alpha)^2\left(\frac{3}{25}\frac{\langle r^4\rangle_{\rho_{ca\beta_2\beta_4}}}{\langle r^2\rangle^2_{\rho_{ca\beta_2\beta_4}}} - \frac{1}{7}\right)\right]}. \quad (17)$$

We would like to note that in Ref. [25], there is a small typing error in the formula for $f(x)$, while in the calculations of Ref. [25], the correct formula from Eq. (19), and Table 2 in Ref. [26] for $f(x)$ was used. While (14) is exact for an arbitrary central potential, provided that E_{FS} is known exactly, (16) is an approximation derived under the assumption of the difference between pointlike and extended potential being a perturbation. The calculation of the ND correction to the bound electron g factor via the effective radius approach

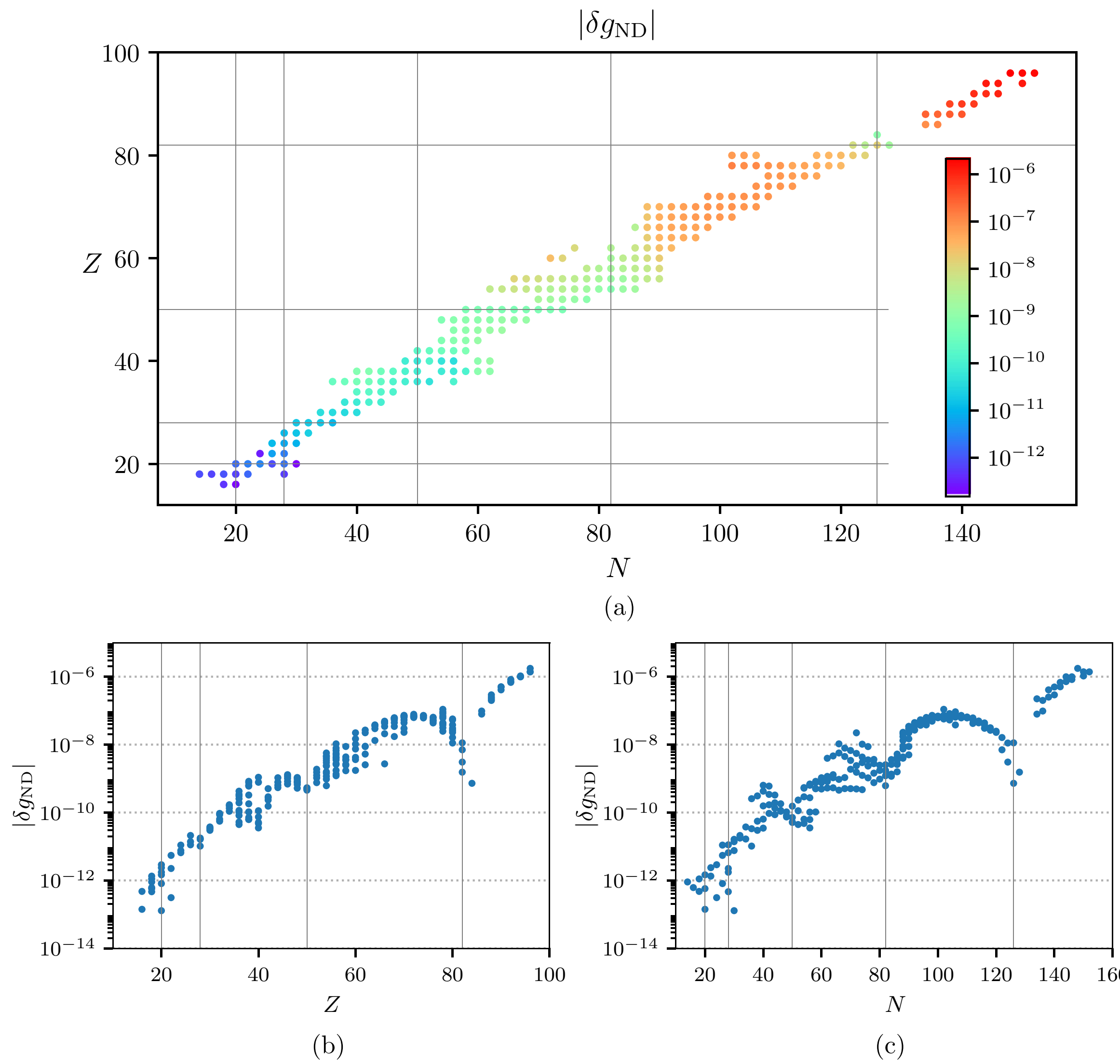

FIG. 1. Nuclear chart with charge number Z and neutron number N, where the gray lines indicate the magic numbers 20, 28, 50, 82, and 126. The points represent even-even nuclei, where their color in panel (a) displays the ND g-factor correction δg_{ND}, which takes particularly low values around the magic numbers and larger values in between. The two lower figures show δg_{ND} for the considered even-even nuclei as a function of only the charge number Z (b) and of only the neutron number N (c), respectively. The vertical solid gray lines are the nuclear magic numbers, which show that filled proton, as well as neutron shells, reduce δg_{ND}.

therefore relies on a perturbative evaluation of the energy derivative in Eq. (14) and is limited by the accuracy of the finite-size corrections.

In this work, the ND g-factor correction is calculated with three methods: First, with the previously used analytical ERM described above. Second, with a numerical ERM, where instead of the approximative Eqs. (16) and (17), Eq. (15) is solved numerically for R and the ND g-factor correction is obtained by using Eq. (7) with the wave functions of the corresponding charged sphere. Finally, we also calculate δg_{ND} nonperturbatively by solving the Dirac equation (3) numerically with the dual kinetic balance method [39] for the potential (2), including all finite-size effects due to the deformed charge distribution $\rho_{ca\beta_2\beta_4}(r,\vartheta)$. Then, the g factors needed in Eq. (11) for the ND correction can be obtained by numerical integration of the wave functions in Eq. (7). Alternatively, the derivative of the energies in Eq. (8) can be calculated numerically as

$$\frac{\partial E_{n\kappa}}{\partial m_e} \approx \frac{E_{n\kappa}^{(m_e+\delta m)} - E_{n\kappa}^{(m_e-\delta m)}}{2\delta m}, \tag{18}$$

with a suitable $\delta m/m_e \ll 1$. Here, $E_{n\kappa}^{(m_i)}$ stands for the binding energy obtained by solving the Dirac equation with the electron mass replaced by m_i. We find both methods to be in excellent agreement.

We calculated the ND g-factor correction for a wide range of even-even, both in the proton and neutron number and therefore spinless, nuclei with charge numbers between 16 and 96 using the deformed Fermi distribution from Eq. (4) with parameters a, c, β_2, and β_4 obtained as described above. The required rms values for the nuclear charge radius are taken from Ref. [36] and the reduced transition probabilities needed for the calculation of β_2 via (13) from Ref. [40]. The resulting values for $|\delta g_{\mathrm{ND}}|$, obtained by the nonperturbative

TABLE I. Comparison of the nuclear deformation g-factor correction obtained by the effective radius method (ERM) with the analytical expressions from Eqs. (16) and (17) ($\delta g_{\rm ND}^{\rm (eff,A)}$) and by the ERM with effective radius and corresponding energy correction calculated numerically ($\delta g_{\rm ND}^{\rm (eff,N)}$) and nonperturbatively by direct numerical calculations ($\delta g_{\rm ND}^{\rm (num)}$) for several isotopes. R_N is the rms nuclear electric charge radius from literature [36] and β_2, β_4 are the deformation parameters of the deformed Fermi distribution (4). The parameters of the deformed Fermi distribution were either taken from Ref. [25] or calculated as described in the text, where the β_4 values from Ref. [38] were used.

	R_N (fm)	β_2	β_4	$\delta g_{\rm ND}^{\rm (eff,A)}$	$\delta g_{\rm ND}^{\rm (eff,N)}$	$\delta g_{\rm ND}^{\rm (num)}$
${}^{58}_{26}$Fe [a]	3.775	0.274	−0.019	-2.10×10^{-11}	-1.95×10^{-11}	-1.99×10^{-11}
${}^{82}_{38}$Sr [a]	4.248	0.263	0.001	-3.57×10^{-10}	-3.16×10^{-10}	-3.27×10^{-10}
${}^{86}_{38}$Sr [b]	4.226	0.134[c]	0.000	-8.98×10^{-11}	-8.01×10^{-11}	-8.24×10^{-11}
${}^{100}_{38}$Sr [b]	4.487	0.435[c]	0.000	-1.08×10^{-09}	-0.97×10^{-09}	-1.00×10^{-09}
${}^{98}_{44}$Ru [a]	4.423	0.194	0.038	-6.91×10^{-10}	-6.02×10^{-10}	-6.21×10^{-10}
${}^{116}_{48}$Cd [a]	4.620	0.190	−0.038	-1.13×10^{-09}	-0.99×10^{-09}	-1.02×10^{-09}
${}^{116}_{50}$Sn [a]	4.625	0.108	−0.008	-5.03×10^{-10}	-4.36×10^{-10}	-4.48×10^{-10}
${}^{134}_{54}$Xe [a]	4.790	0.113	0.000	-1.09×10^{-09}	-0.94×10^{-09}	-0.96×10^{-09}
${}^{142}_{60}$Nd [b]	4.912	0.100	0.000	-2.01×10^{-09}	-1.71×10^{-09}	-1.76×10^{-09}
${}^{150}_{60}$Nd [b]	5.042	0.278	0.000	-1.70×10^{-08}	-1.45×10^{-08}	-1.49×10^{-08}
${}^{144}_{62}$Sm [b]	4.945	0.090	0.000	-2.14×10^{-09}	-1.81×10^{-09}	-1.85×10^{-09}
${}^{154}_{62}$Sm [b]	5.111	0.328	0.000	-3.24×10^{-08}	-2.75×10^{-08}	-2.82×10^{-08}
${}^{152}_{64}$Gd [a]	5.077	0.202	0.050	-1.86×10^{-08}	-1.56×10^{-08}	-1.60×10^{-08}
${}^{208}_{82}$Pb [a]	5.501	0.061	0.000	-1.35×10^{-08}	-1.10×10^{-08}	-1.13×10^{-08}
${}^{234}_{92}$U [b]	5.829	0.256	0.080	-1.12×10^{-06}	-0.90×10^{-06}	-0.91×10^{-06}
${}^{238}_{92}$U [b]	5.851	0.280	0.070	-1.28×10^{-06}	-1.02×10^{-06}	-1.04×10^{-06}
${}^{244}_{94}$Pu [a]	5.895	0.284	0.062	-1.57×10^{-06}	-1.25×10^{-06}	-1.27×10^{-06}
${}^{248}_{96}$Cm [a]	5.869	0.294	0.040	-1.90×10^{-06}	-1.51×10^{-06}	-1.54×10^{-06}

[a] Parameters obtained as described in the text.
[b] Parameters of deformed Fermi distribution taken from Ref. [25].
[c] Value from Ref. [42].

method, are shown in Fig. 1 as a function of the charge number Z and the neutron number N. If proton or neutron number is in the proximity of a nuclear magic number 2, 8, 20, 28, 50, 82, and 126, which corresponds to a filled proton or neutron shell [41], the nuclear shell closure effects also transfer to the bound electron g factor, and the ND correction is reduced. In Table I, a comparison between our numerical approaches and the analytical ERM from Ref. [25] is shown. The β_2 parameters for ^{86,100}Sr are taken from Ref. [42], which was not specified in Ref. [25].

Now, let us discuss the main causes for the disagreement of the results as presented in Table I. Both Eqs. (16) and (17) are approximations derived by perturbation theory, which affects the accuracy of the analytical ERM ($\delta g_{\rm ND}^{\rm (eff,A)}$). Equation (16) has an estimated relative uncertainty $\lesssim 0.2\%$ [26] and (17) uses only the second and fourth moments of the nuclear charge distribution for finding the effective radius. Also, it was shown in Ref. [28] that the analytical ERM for arbitrary charge distributions is incomplete in order $(Z\alpha)^2 m_e (Z\alpha m_e R_N)^3$, where R_N is the nuclear rms charge radius. Furthermore, even if the effective radius is calculated without approximations according to Eq. (15), the wave functions of the corresponding homogeneously charged sphere differ slightly from the ones of the deformed Fermi distribution with the same binding energy. This affects values of the g factor and explains the difference between the numerical ERM ($\delta g_{\rm ND}^{\rm (eff,N)}$) and the direct numerical calculations ($\delta g_{\rm ND}^{\rm (num)}$). Finally, being a difference of two small finite-nuclear-size corrections, the ND correction can exhibit enhanced sensitivity on the uncertainty of the ERM. From Table I, we conclude that for high Z, the difference between analytical ERM and nonperturbative calculations is mainly due to the approximations in Eqs. (16) and (17).

Concluding, the analytical ERM proved to be a good order-of-magnitude estimate of the ND correction, but for high-precision calculations, nonperturbative methods beyond the ERM and without an expansion in $Z\alpha$ or $Z\alpha\, m_e\, R_N$ are indispensable. Convergence of the numerical methods was checked by varying numerical parameters and using various grids, and the obtained accuracy permits the consideration of nuclear size and shape with an accuracy level much higher than the differences to the perturbative method for the considered nuclei. For low-Z nuclei, however, it becomes increasingly difficult to resolve the small deformation effect with the numerical methods.

IV. CONCLUSION

In summary, the ND g-factor correction was calculated nonperturbatively for a wide range of nuclei by using quadrupole deformations estimated from nuclear data. By comparing the previously used perturbative ERM and the all-order numerical approach, it was shown that the contributions of the nonperturbative effects can amount up to the 20% level. Previously, the uncertainty of the finite nuclear size correction was commonly estimated as the difference between the Fermi distribution and a homogeneously charged sphere, which is a very conservative estimate [9]. If the finite size correction is calculated including deformation effects, the remaining model uncertainty is reduced to the difference between the deformed Fermi distribution and the true, unknown nuclear charge distribution. As a consequence, precise calculation of deformation effects are needed. In the low-Z regime, the ND corrections can safely be neglected, especially for the ions considered in Ref. [1]. However, considering a ND correction up to the parts-per-million level and an expected parts-per-billion accuracy, or even below, for the g-factor experiments with high-Z nuclei, in this case an all-order treatment is indispensible. These results motivate a nonperturbative treatment of nuclear shape effects also for other atomic properties, e.g., fine and hyperfine splittings. The distribution of electric charge inside the nucleus is a major theoretical uncertainty for g factors with heavy nuclei, which suggests the extraction of information thereon from experiments. Our work demonstrates the required accurate mapping of arbitrary nuclear charge distributions to corresponding g factors. Furthermore, the ND correction was shown to be a not monotonically increasing function of the nuclear charge number. In fact, it rather reflects the nuclear shell model by taking particularly low values around filled proton, as well as neutron shells, showing the neutrons' indirect influence on the distribution of electric charge inside the atomic nucleus.

ACKNOWLEDGMENTS

The authors acknowledge insightful conversations with Z. Harman and V. Debierre.

[1] S. Sturm, F. Köhler, J. Zatorski, A. Wagner, Z. Harman, G. Werth, W. Quint, C. Keitel, and K. Blaum, Nature (London) **506**, 467 (2014).
[2] H. Haffner, T. Beier, N. Hermanspahn, H.-J. Kluge, W. Quint, S. Stahl, J. Verdu, and G. Werth, Phys. Rev. Lett. **85**, 5308 (2000).
[3] J. Verdu, S. Djekic, H. Haffner, S. Stahl, T. Valenzuela, M. Vogel, G. Werth, H.-J. Kluge, and W. Quint, Phys. Rev. Lett. **92**, 093002 (2004).
[4] F. Köhler, S. Sturm, A. Kracke, G. Werth, W. Quint, and K. Blaum, J. Phys. B: At. Mol. Opt. Phys. **48**, 144032 (2015).
[5] J. Zatorski, B. Sikora, S. G. Karshenboim, S. Sturm, F. Köhler-Langes, K. Blaum, C. H. Keitel, and Z. Harman, Phys. Rev. A **96**, 012502 (2017).
[6] S. Sturm, A. Wagner, B. Schabinger, J. Zatorski, Z. Harman, W. Quint, G. Werth, C. H. Keitel, and K. Blaum, Phys. Rev. Lett. **107**, 023002 (2011).
[7] F. Köhler, K. Blaum, M. Block, S. Chenmarev, S. Eliseev, D. A. Glazov, M. Goncharov, J. Hou, A. Kracke, D. A. Nesterenko *et al.*, Nat. Commun. **7**, 10246 (2016).
[8] V. A. Yerokhin, K. Pachucki, Z. Harman, and C. H. Keitel, Phys. Rev. Lett. **107**, 043004 (2011).
[9] G. Werth, H. Häffner, N. Hermanspahn, H.-J. Kluge, W. Quint, and J. Verdú, in *The Hydrogen Atom: Precision Physics of Simple Atomic Systems*, edited by S. G. Karshenboim, F. Bassani, F. Pavone, M. Inguscio, and T. Hänsch (Springer, Berlin, 2001), pp. 204–220.
[10] V. M. Shabaev, D. A. Glazov, N. S. Oreshkina, A. V. Volotka, G. Plunien, H.-J. Kluge, and W. Quint, Phys. Rev. Lett. **96**, 253002 (2006).
[11] V. A. Yerokhin, E. Berseneva, Z. Harman, I. I. Tupitsyn, and C. H. Keitel, Phys. Rev. Lett. **116**, 100801 (2016).
[12] H.-J. Kluge, T. Beier, K. Blaum, L. Dahl, S. Eliseev, F. Herfurth, B. Hofmann, O. Kester, S. Koszudowski, C. Kozhuharov *et al.*, in *Current Trends in Atomic Physics*, edited by S. Salomonson and E. Lindroth, Advances in Quantum Chemistry Vol. 53 (Academic Press, New York, 2008), pp. 83–98.
[13] M. Vogel, Z. Andelkovic, G. Birkl, S. Ebrahimi, V. Hannen, D. von Lindenfels, A. Martin, T. Murböck, W. Nörtershäuser, W. Quint *et al.*, Phys. Scr. **T166**, 014066 (2015).
[14] S. Sturm, M. Vogel, F. Köhler-Langes, W. Quint, K. Blaum, and G. Werth, Atoms **5**, 4 (2017).
[15] V. A. Yerokhin, P. Indelicato, and V. M. Shabaev, Phys. Rev. A **69**, 052503 (2004).
[16] V. A. Yerokhin and Z. Harman, Phys. Rev. A **95**, 060501 (2017).
[17] K. Pachucki, A. Czarnecki, U. D. Jentschura, and V. A. Yerokhin, Phys. Rev. A **72**, 022108 (2005).
[18] V. A. Yerokhin and Z. Harman, Phys. Rev. A **88**, 042502 (2013).
[19] A. Czarnecki and R. Szafron, Phys. Rev. A **94**, 060501 (2016).
[20] A. Czarnecki, M. Dowling, J. Piclum, and R. Szafron, Phys. Rev. Lett. **120**, 043203 (2018).
[21] A. V. Nefiodov, G. Plunien, and G. Soff, Phys. Rev. Lett. **89**, 081802 (2002).
[22] A. V. Volotka and G. Plunien, Phys. Rev. Lett. **113**, 023002 (2014).
[23] S. G. Karshenboim, Phys. Lett. A **266**, 380 (2000).
[24] D. A. Glazov and V. M. Shabaev, Phys. Lett. A **297**, 408 (2002).
[25] J. Zatorski, N. S. Oreshkina, C. H. Keitel, and Z. Harman, Phys. Rev. Lett. **108**, 063005 (2012).
[26] V. M. Shabaev, J. Phys. B: At. Mol. Opt. Phys. **26**, 1103 (1993).
[27] Y. S. Kozhedub, O. V. Andreev, V. M. Shabaev, I. I. Tupitsyn, C. Brandau, C. Kozhuharov, G. Plunien, and T. Stöhlker, Phys. Rev. A **77**, 032501 (2008).
[28] S. G. Karshenboim and V. G. Ivanov, Phys. Rev. A **97**, 022506 (2018).
[29] W. Greiner, *Relativistic Quantum Mechanics*, 3rd ed. (Springer-Verlag, Berlin, 2000).
[30] D. Hitlin, S. Bernow, S. Devons, I. Duerdoth, J. W. Kast, E. R. Macagno, J. Rainwater, C. S. Wu, and R. C. Barrett, Phys. Rev. C **1**, 1184 (1970).
[31] Y. Tanaka, R. M. Steffen, E. B. Shera, W. Reuter, M. V. Hoehn, and J. D. Zumbro, Phys. Rev. C **29**, 1830 (1984).
[32] B. Hahn, D. G. Ravenhall, and R. Hofstadter, Phys. Rev. **101**, 1131 (1956).
[33] T. Beier, Phys. Rep. **339**, 79 (2000).
[34] S. G. Karshenboim, R. N. Lee, and A. I. Milstein, Phys. Rev. A **72**, 042101 (2005).
[35] G. Breit, Nature (London) **122**, 649 (1928).
[36] I. Angeli and K. Marinova, At. Data Nucl. Data Tables **99**, 69 (2013).
[37] F. Träger, Zeitschr. Phys. A **299**, 33 (1981).

[38] P. Möller, J. R. Nix, W. D. Myers, and W. J. Swiatecki, At. Data Nucl. Data Tables **59**, 185 (1995).

[39] V. M. Shabaev, I. I. Tupitsyn, V. A. Yerokhin, G. Plunien, and G. Soff, Phys. Rev. Lett. **93**, 130405 (2004).

[40] Evaluated nuclear structure data file (ensdf), http://www.nndc.bnl.gov/ensdf/

[41] P. Ring and P. Schuck, *The Nuclear Many-Body Problem* (Springer-Verlag, Berlin, 1980).

[42] F. Buchinger, E. B. Ramsay, E. Arnold, W. Neu, R. Neugart, K. Wendt, R. E. Silverans, P. Lievens, L. Vermeeren, D. Berdichevsky *et al.*, Phys. Rev. C **41**, 2883 (1990).